Last 150 kyr volcanic activity on Mauritius island (Indian ocean) revealed by new Cassignol-Gillot unspiked K–Ar ages

Xavier Quidelleur, Vincent Famin

Quaternary Geochronology 82 (2024) 101534

Contents lists available at ScienceDirect

Quaternary Geochronology

journal homepage: www.elsevier.com/locate/quageo

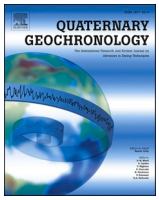

Last 150 kyr volcanic activity on Mauritius island (Indian ocean) revealed by new Cassignol-Gillot unspiked K–Ar ages

Xavier Quidelleur [a,*], Vincent Famin [b,c]

[a] Université Paris-Saclay, CNRS, GEOPS, Orsay, 91405, France
[b] Université Paris Cité, Institut de Physique du Globe de Paris, CNRS, UMR 7154, Paris, 75005, France
[c] Université de La Réunion, Laboratoire GéoSciences Réunion, Saint Denis, 97744, France

ARTICLE INFO

Keywords:
Indian ocean
Mauritius island
Unspiked K–Ar
Pre-Holocene

ABSTRACT

We present new K–Ar ages extending the volcanic history of Mauritius Island towards the Holocene. Mauritius volcanism is associated with the activity of the Réunion hotspot, the magmatism of which produced the Deccan Traps across the Cretaceous-Tertiary (KT) boundary and continues up to present on Réunion Island. After shield building from before 8.9 Ma to 4.7 Ma, Mauritius Island underwent an unusual volcanic evolution involving two rejuvenation stages (3.5–1.9 Ma and <0.7 Ma) separated by a 1.2 Myr hiatus. The lower bound of the second rejuvenation stage being poorly constrained, it is not clear whether volcanism in this island has come to a rest. Given the occurrence of uneroded, and yet undated strombolian cones in Mauritius, it is important to better constrain the latest activity of this island in order to assess its volcanic hazard. The importance of dating the end of this stage is also enhanced by the fact that most of the surface of Mauritius is covered by the lavas of the rejuvenation stages, hence indicating a recent volcanic activity that needs to be better characterized for risk assessment.

We focus here on the last 150 ka interval which lacked precise age controls with only a few whole-rock and groundmass $^{40}Ar/^{39}Ar$ plateau ages available (Moore et al., 2011), ranging from 138 ± 29 to 40 ± 48 ka (uncertainties are 1 σ). Our six new Cassignol-Gillot unspiked K–Ar ages obtained on plagioclase or groundmass range from 113 ± 7 to 14 ± 3 ka, with much lower uncertainties than previous ages available. Our major and trace element analyses of the dated samples highlight the compositional homogeneity of the lavas erupted in the last rejuvenation stage, showing no geochemical evolution.

Our results, with ages as young as 14 ± 3 ka, demonstrate that near-Holocene volcanism is present in Mauritius Island, with no evidence of fading magmatism in the last 150 ka. Our second youngest age at 44 ± 5 ka implies that the latest activity occurred after a ~30 kyr repose interval, with the consequence that Mauritius volcanism may resume at any time.

1. Introduction

The island of Mauritius is one of the latest volcanic manifestations of the Réunion hotspot (e.g., Morgan, 1981). This hotspot is materialized by a trail of magmatism running on the Indian plate from the Deccan traps erupted ca. 65 Ma ago to the Maldives (~58 Ma) and Chagos (~50 Ma) archipelagoes, then jumping on the Somali plate from the Mascarene plateau (50–30 Ma) to Mauritius (<9 Ma) and Réunion (<5 Ma) islands. As for many hotspot volcanic islands, Mauritius experienced a main construction stage, called shield building, from 9 to 4.7 Ma (McDougall and Chamalaun, 1969; Moore et al., 2011), presumably at the apex of rising plume magmas. Then, the northward displacement of the oceanic lithosphere moved the island away from the main magma supply source, and volcanism halted for 1.2 Myr. Note that all the ages hereafter are expressed relative to the FCT-3 biotite standard at 28.03 Ma and calculated with the decay constants of Steiger and Jäger (1977).

About 3.5 Ma ago, volcanism on Mauritius resumed. Rejuvenescent (also referred to as post-erosional) volcanism is common in archipelagoes associated with mantle-plumes, including Hawai'i, the Canaries, and Samoa (e.g., Guillou et al., 2004; Konter and Jackson, 2012), occurring after rests of up to 2.1 Myr (e.g., Garcia et al., 2016), and lasting for up to 2.5 Myr (e.g., Garcia et al., 2010). The origin of

* Corresponding author.
E-mail address: xavier.quidelleur@universite-paris-saclay.fr (X. Quidelleur).

https://doi.org/10.1016/j.quageo.2024.101534
Received 17 August 2023; Received in revised form 12 April 2024; Accepted 30 April 2024
Available online 3 May 2024

rejuvenescent magmatism is still debated, with many proposed hypotheses such as mantle decompression caused by lithospheric bend under the load of the edifices (Bianco et al., 2005), or late melting of the more depleted distal upper part of the plume (Paul et al., 2005). The case of Mauritius, however, is particularly intriguing because this island experienced two periods of rejuvenescent volcanism (Simpson, 1950; Baxter, 1972, 1976; Perroud, 1982), one from 3.5 to 1.9 Ma and another since <0.7 Ma.

Although there is consensus about the beginning of rejuvenescent volcanism in Mauritius, considerable uncertainty exists about the timing of its cessation. The seminal study of McDougall and Chamalaun (1969) proposed a last activity of Mauritius at 177 ± 7 ka based on whole-rock K–Ar ages (all uncertainties are 1 σ, unless otherwise stated), whereas Moore et al. (2011) obtained ages as young as 40 ± 48 ka based on the $^{40}Ar/^{39}Ar$ technique on groundmass. Other studies mention even younger ages of 31 ka from K–Ar on groundmass (Nohda et al., 2005), or 25 ka from ^{14}C (Saddul, 2002), but without providing the data nor even the uncertainties on these ages, which make them unusable in any volcanic hazard assessment. Given the 0–185 kyr uncertainty about the cessation of activity in Mauritius, the duration of its rejuvenescent volcanism is not precisely known, nor is the probability of future eruptions on this island.

The objective of the present study is to fill this gap in knowledge, by providing more precise geochronological information on the most recent volcanic morphologies of Mauritius Island, in order to better constrain the duration of the rejuvenescent stage of the island. To do so, we employed K–Ar dating on groundmass with the Cassignol-Gillot technique (Cassignol and Gillot, 1982), targeting the least eroded volcanic features of the island. Combined with major and trace element analyses, our new ages considerably improve the recent geological history of Mauritius and allow us to assess the recurrence of eruptions for the past 150 ka and the volcanic hazard of the island.

2. Geological setting

The geological history of subaerial Mauritius is generally subdivided into three periods of eruptive activity separated by volcanic quiescence and erosion (Simpson, 1950; Baxter, 1972, 1976; Perroud, 1982). The Older series (>8.9–4.7 Ma) corresponds to the shield building stage of the island. It is made of transitional basalts with relatively low crystal fractionation (Baxter, 1975), and an isotopic signature enriched in ^{3}He and radiogenic isotopes indicative of a mantle plume contribution (Hanyu et al., 2001; Paul et al., 2005, 2007; Moore et al., 2011; Nauret et al., 2019). The Older series ended with the emplacement of highly differentiated trachytes containing Archean zircons (Ashwal et al., 2016, 2017), interpreted as derived from partial melting of a mantle contaminated by recycled continental crust (Ashwal et al., 2017; Nauret et al., 2019).

The two periods of rejuvenescent volcanism have been called the Intermediate (3.5–1.8 Ma) and Younger series (<1 Ma), respectively (Baxter, 1972, 1976; Perroud, 1982). They are distinguished from the Older series by being more alkaline in composition and more depleted in radiogenic isotopes due to the dominant contribution of MORB mantle in magmas (Paul et al., 2005, 2007; Moore et al., 2011; Nauret et al., 2019). Lavas from the two latter series are interpreted as evidence for a slightly lower degree of partial melting as suggested from their incompatible element abundances (Paul et al., 2005). The Younger series erupted K-poor alkaline olivine basalts and basanites from strombolian craters aligned along an overall N20°E direction forming the central crest of Mauritius Island (Fig. 1).

Due to the intense erosion under tropical climate, remains of the Older series are rather limited and represent a small fraction of the outcropping volcanism (Fig. 1c). On the other hand, the Intermediate series outcrops over all the island, while the Younger series covers about half of Mauritius' surface (Giorgi et al., 1999). Moore et al. (2011) suggested that the total area covered by the Younger series might actually cover most of the island. However, core analysis showed that the total cover deposited by the two rejuvenescent periods of volcanism is in fact very thin, amounting to less than 0.1% of the whole volcano volume built onto the ocean floor (Moore et al., 2011).

3. Methods

Samples were collected in 2019 at six localities corresponding to uneroded volcanic morphologies, such as well-preserved volcanic cones or flat lava flows without significant soil developed on them. Sampling sites were further chosen for their complementarity with previous dating studies, or to allow comparison with published ages. For instance, our sample 19MU10 was taken on the same lava flow as samples MR95-11 (88 ka) and MR95-14 (124 ka) from Nohda et al. (2005) and is nearly equidistant to these samples. Similarly, our sample 19MU02 was collected close to M33 (44 ± 36 ka) and B6-3 (40 ± 48 ka) by Moore et al. (2011), all located on the same uppermost lava flow of the area. Finally, our sample 19MU07 comes from the same location as M15 (56 ± 36 ka) previously dated by Moore et al. (2011). Great care was taken to collect only hand-size blocks from the inner part of massive lavas, because the absence of visible alteration and vesicularity are two criteria of paramount importance for the quality and precision of dating results by the K–Ar method.

3.1. K–Ar dating

Thin sections were examined to validate the selection of samples suitable for dating according to the absence of alteration and vesicles, and also to determine the most appropriate phases and size fractions to be used for K–Ar dating. Whenever possible, groundmass was preferred for dating because it crystallized during the cooling of erupted lavas. However, due to the rock texture (Supp. Mat. 1) of samples 19MU02 and 19MU10 which lack groundmass fraction, plagioclase crystals were selected within the 80–125 and 125–250 μm size fractions, respectively. Groundmass within the 125–250 μm size fraction was preferred for samples 19MU07, 19MU09 and 19MU14, while the groundmass size 80–125 μm was selected for sample 19MU03 which displays a higher glass content (Supp. Mat. 1). Following ultrasonic cleaning in de-ionized water, diiodomethane was used to isolate a narrow density range of the groundmass or plagioclase fraction. By selecting the heaviest fraction of the groundmass, or of the plagioclase crystals, we have an additional guaranty that, if any, the weathered portion of them would be eliminated. Indeed, because weathering tends to transform crystals or groundmass into clays, they are lighter than the fresh fraction. Consequently, our density separation helps us to further eliminate possible undetected traces of weathering.

We performed unspiked K–Ar analyses at the GEOPS laboratory (Université Paris-Saclay, France) following the Cassignol-Gillot technique (Cassignol and Gillot, 1982; Gillot and Cornette, 1986; Gillot et al., 2006). Note that the conventional K–Ar technique, which is based on the isotopic dilution approach using an ^{38}Ar spike with a known number of atoms, is no longer used due to its limitation for dating young (<0.1 Ma) rocks with low (<5%) radiogenic content. On the other hand, because of the very stable analytical conditions reached during ^{40}Ar and ^{36}Ar analyses, the Cassignol-Gillot technique allows rocks as young as a few ka to be dated (e.g., Quidelleur et al., 2001). This technique has a demonstrated record of successful dating up to the Holocene realm, and an excellent consistency with stratigraphy, geology (e. g. Rusquet et al., 2023) and other dating techniques, (e.g., ^{14}C, Quidelleur et al., 2022; (U–Th)/He on zircon, Famin et al., 2022).

Potassium (K) and argon (Ar) concentration measurements were triplicated (19MU10) or duplicated (other samples) on different aliquots following the procedure and uncertainties calculation described in detail in Germa et al. (2011). Potassium content was determined by flame spectroscopy using an Agilent AA240 spectrometer operating in absorption mode. Measurements were calibrated using K solutions with

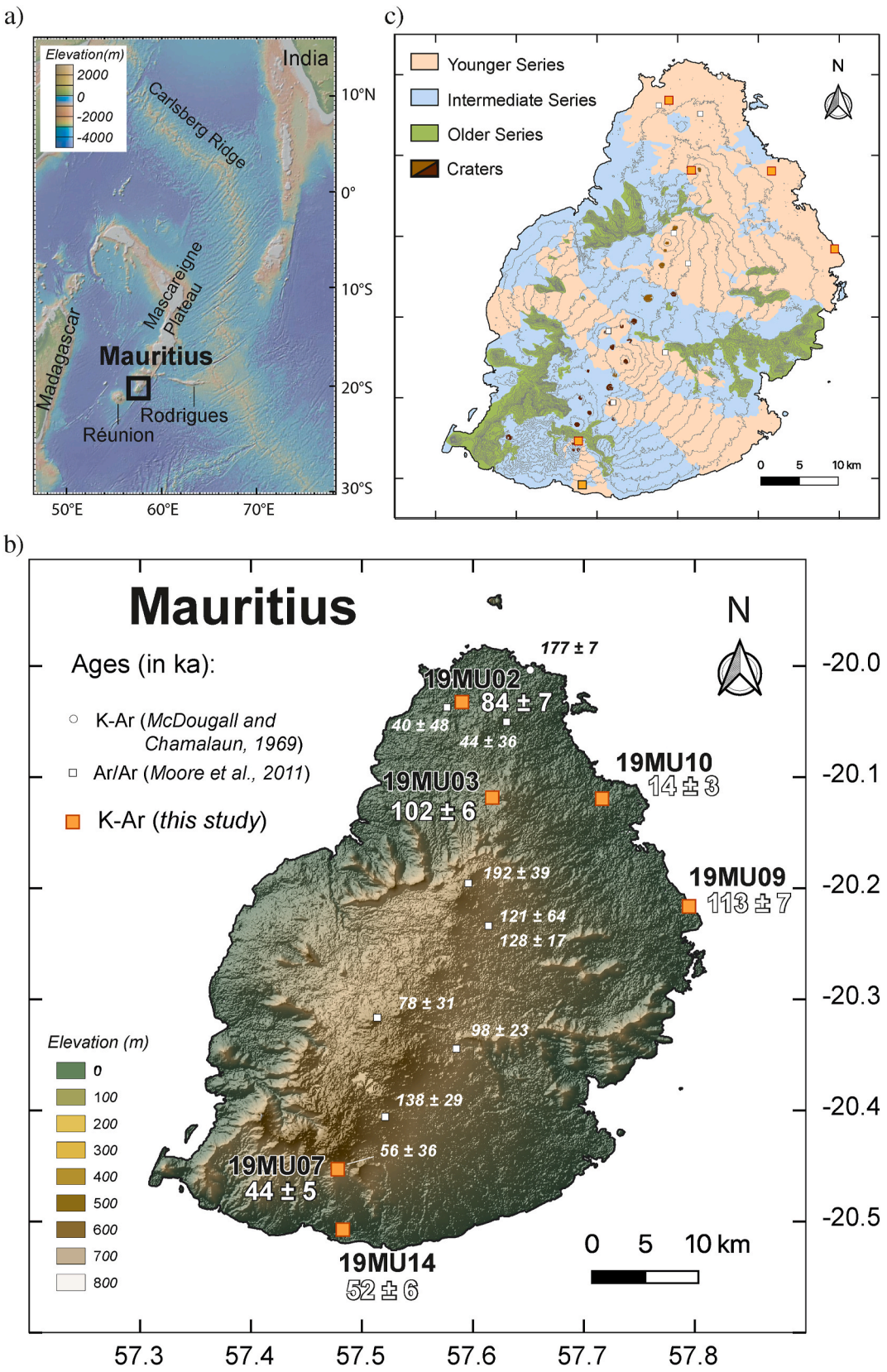

Fig. 1. a) Top-left: setting of Mauritius Island within the Indian Ocean and its location relative to India and Madagascar. Image made using GeoMapApp. b) Bottom: Location map of dated samples from this (orange symbols) and previous (white symbols) studies. Ages and uncertainties are given in ka. The shaded digital elevation model of Mauritius was drawn using QGIS software and topographic data are from the Japan Aerospace Exploration Agency. c) Top-right: Simplified geology map of Mauritius Island (modified from Baxter, 1972; Giorgi et al., 1999; Moore et al., 2011) showing the main outcrops of the Older (green), Intermediate (blue), and Younger (beige) Series, as well as dated samples from b) plotted using the same symbols.

concentration ranging from 1 to 2 mg/l and compared to reference standards MDO-G (K = 3.510%; Gillot et al., 1992) and BCR-2 (K = 1.481%; Raczek et al., 2001). Argon was measured using a multi-collector 180° sector mass spectrometer in three different steps. First, an atmospheric argon aliquot from an air pipette was analyzed for ^{40}Ar signal calibration. This air pipette was calibrated by routine measurements of HD-B1 standard (Fuhrmann et al., 1987) using the age of 24.18 Ma (Schwarz and Trieloff, 2007). Second, after complete extraction by fusion above 1500 °C, Ar isotopes from the sample were measured after complete purification with high temperature Ti foam and SAES getters operated at 350 °C. Third, another air pipette, with the same ^{40}Ar signal as the sample to be dated, was measured in order to perform an accurate atmospheric correction.

The age is calculated using the K isotopic ratios and ^{40}K decay constants of Steiger and Jäger (1977). The mean age is obtained by weighted mean calculation (Taylor, 1982) of the replicated Ar analyses. All uncertainties reported in this study are quoted at the 1σ level. Accordingly, all the uncertainties on literature ages have been converted to 1σ to allow the comparison of new and published geochronological data.

3.2. Major and trace elements

Whole-rock samples were finely powdered in an agate mortar. Major and trace elements measurements were conducted at the University of Bretagne Occidentale (Brest, France) via ICP-AES (Thermo Electron IRIS Advantage) and ICP-MS (Thermo Elemental x7). Prior to analysis, samples were fused with $LiBO_2$ in Pt–Au crucibles before being dissolved with HNO_3. International standards used for calibration (BCR-2 and BHVO-2) underwent the same process as samples (Carignan et al., 2001). Relative 2 σ uncertainties are lower than 2% for major elements and lower than 5% for trace elements.

4. Results

4.1. K–Ar dating

We have obtained six new K–Ar ages ranging from 113 ± 7 to 14 ± 3 ka (Table 1 and Fig. 1c). Potassium content ranges from 0.208% to 0.344% for the groundmass, and from 0.241% to 0.292% for plagioclase crystals. Radiogenic argon contents are lower than 1.5%, with values as low as 0.16%–0.36% for 19MU10, our youngest sample. To further support its age, a third Ar measurement has been performed. All three determinations are undistinguishable at the 1 σ level, leading to a weighted-mean age of 14 ± 3 ka for 19MU10 (Table 1). Note that plagioclase crystals of samples 19MU01 and 19MU10 do not present reaction rims (Supp. Mat. 1) supporting the hypothesis that they are not xenocrysts incorporated in the magma before the eruption without having stayed long enough for Ar to diffuse out (e.g., Germa et al., 2023). We thus consider here these plagioclases as juvenile and their age date the timing of eruption.

4.2. Geochemistry

Major and trace elements analyses for rocks from this study are provided in Table 2. For the sake of comparison, we have completed our major and trace elements dataset using the GEOROC database with previous analyses from Baxter (1975), Sheth et al. (2003), Nohda et al. (2005), Paul et al. (2005, 2007), and Moore et al. (2011).

The total alkali versus silica (TAS) diagram (Fig. 2) shows that our six samples are within the field of alkali basalts or close to it. They have low SiO_2 and alkali contents, as also observed for all lavas from the Younger series of Mauritius.

Diagram of Rare Earth Elements (REE) normalized to chondrite and Spider diagrams of trace elements normalized to the primitive mantle (Sun and McDonough, 1989) are also shown in Fig. 3. Rocks from this study are within the field of the Younger series. Samples 19MU02, 19MU03, 19MU10, and 19MU14 display very close trace element compositions, while 19MU07 and 19MU09 are slightly enriched and depleted compared to the other samples, respectively.

5. Discussion

5.1. Comparison with previous ages

The first absolute chronology of Mauritius was made by McDougall and Chamalaun (1969) based on whole-rock K–Ar dating, who established that the Younger Series spanned from 0.71 to 0.18 Ma (after recalculation of ages using the constants of Steiger and Jäger, 1977), without any age being younger than 150 ka. More recently, Moore et al. (2011) reported 20 ^{40}Ar/^{39}Ar ages obtained from groundmass or whole-rock on borehole and surface samples from the Younger series, including eight ages younger than 150 ka. Note that these ages were obtained using the FCT-3 biotite with an age of 28.03 Ma as a neutron flux monitor, allowing a direct comparison with our K–Ar ages calibrated with HD-B1 at 24.18 Ma (Schwarz and Trieloff, 2007). Seven K–Ar whole-rock ages, ranging from 0 ± 120 to 1000 ± 25 ka, were also provided by Moore et al. (2011) for the Younger series, but without any description regarding the analytical procedures or the reproducibility of the data. In addition, 12 K–Ar ages for the Younger series are given by Nohda et al. (2005), but as they lack uncertainty and description, we cannot consider them further for interpretation purposes. Finally, six

Table 1
New K–Ar ages performed on groundmass or plagioclase separates. Column headings indicate sample names; latitude (in degrees); longitude (degrees); mean potassium (K) concentration in percent; concentration of radiogenic ^{40}Ar (^{40}Ar*) in percent; concentration of radiogenic ^{40}Ar (^{40}Ar*) × 10^{10} in number of atoms per gram; age (in Ma); 1-sigma uncertainty (Un., in Ma); weighted mean age (in Ma) calculated from triplicate (19MH10) or duplicate (other samples) analyses shown as different lines; 1-sigma weighted uncertainty (in Ma).

Sample (phase)	Lat. (°)	Long. (°)	K (%)	^{40}Ar* (%)	^{40}Ar* (10^{10} at/g)	Age (Ma)	Un. (Ma)	Mean age (Ma)	±1 σ (Ma)
19MU02	−20.031526	57.588884	0.292	0.72	2.4890	0.082	0.011		
(plagioclase)				1.05	2.5796	0.085	0.008	**0.084**	**0.007**
19MU03	−20.118315	57.616867	0.339	1.21	3.5959	0.102	0.008		
(groundmass)				1.25	3.6449	0.103	0.008	**0.102**	**0.006**
19MU07	−20.453595	57.477463	0.478	0.62	2.3866	0.048	0.008		
(groundmass)				0.62	2.0640	0.041	0.007	**0.044**	**0.005**
19MU09	−20.215781	57.794458	0.208	0.97	2.2471	0.103	0.011		
(groundmass)				1.48	2.5855	0.119	0.008	**0.113**	**0.007**
19MU10	−20.215781	57.716194	0.241	0.28	0.42537	0.017	0.006		
(plagioclase)				0.16	0.23346	0.009	0.006		
				0.36	0.36470	0.014	0.004	**0.014**	**0.003**
19MU14	−20.507954	57.481774	0.344	0.52	1.6857	0.047	0.009		
(groundmass)				0.65	2.0767	0.058	0.009	**0.052**	**0.006**

Table 2
Major (in %) and trace elements (in ppm) composition of whole-rock samples dated here. L.O.I: loss on ignition.

	19MU02	19MU03	19MU07	19MU09	19MU10	19MU14
Wt.%						
SiO_2	47.36	47.13	44.91	46.44	46.75	45.55
TiO_2	1.73	1.79	2.02	1.53	1.62	1.72
Al_2O_3	16.14	16.25	14.72	15.06	15.07	14.92
Fe_2O_3	12.98	13.15	14.22	13.87	13.41	14.12
MnO	0.18	0.18	0.19	0.18	0.18	0.19
MgO	8.98	8.70	10.70	11.71	10.55	11.77
CaO	10.87	11.02	10.10	9.75	9.97	10.02
Na_2O	2.92	3.01	3.10	2.61	2.80	2.92
K_2O	0.31	0.34	0.51	0.20	0.30	0.38
P_2O_5	0.17	0.18	0.23	0.12	0.15	0.18
L.O.I.	−0.81	1.41	−0.08	−0.64	−0.64	−0.36
Total	99.50	100.70	100.63	100.99	101.10	101.13
ppm						
Ba	75.5	80.8	123.6	48.4	73.3	85.7
Ce	18.2	19.5	27.7	13.4	18.0	20.4
Co	55.6	55.1	64.0	69.6	59.8	68.7
Cr	320	296	384	456	395	396
Cu	77.3	83.0	81.4	62.9	89.5	84.8
Dy	3.75	3.92	3.97	3.44	3.67	3.62
Er	1.93	2.04	2.00	1.85	1.92	1.89
Eu	1.23	1.28	1.48	0.99	1.17	1.24
Gd	3.64	3.83	4.27	3.19	3.45	3.60
Hf	2.14	2.25	2.69	1.73	2.04	2.21
Ho	0.74	0.78	0.77	0.70	0.73	0.72
K	2473	2735	3883	2066	2448	3077
La	8.05	8.72	12.74	5.61	7.72	9.14
Lu	0.26	0.26	0.26	0.23	0.25	0.25
Mn	1387	1411	1495	1450	1369	1493
Mo	0.64	0.61	0.72	0.65	0.43	0.64
Nb	10.89	11.83	18.5	6.98	11.1	12.6
Nd	12.1	12.9	16.9	9.3	11.8	13.2
Ni	166	152	279	349	271	325
P	745	809	1080	994	738	797
Pb	0.712	0.775	1.086	0.466	0.640	0.782
Pr	2.55	2.74	3.75	1.94	2.59	2.83
Rb	5.64	5.65	9.78	2.77	4.55	7.29
Sm	3.13	3.35	4.00	2.59	3.09	3.29
Sr	229	230	284	207	193	236
Ta	0.67	0.72	1.1	0.42	0.6	0.7
Tb	0.64	0.67	0.71	0.56	0.62	0.62
Th	0.88	0.97	1.33	0.56	0.72	0.90
Ti	10983	11189	12638	13909	9915	10968
Tm	0.28	0.29	0.29	0.41	0.28	0.27
U	0.22	0.22	0.33	0.13	0.19	0.24
V	263	266	268	261	237	255
Y	18.88	19.81	19.53	19.05	18.70	18.01
Yb	1.79	1.87	1.84	1.62	1.75	1.74
Zn	103	105	112	110	99	110
Zr	84.6	91.2	117.8	69.2	85.9	90.0

Sup. Mat. 1: Thin sections, with plane-polarized light on top and cross-polarized light below, for each sample from this study.

K–Ar whole-rock ages of the Younger series are also available in Montaggioni and Martin-Garin (2020), none of them being younger than 150 ka.

After rejecting the ages of Nohda et al. (2005) because of their lack of uncertainties, two samples from our study may be compared to previously dated samples. To the north of the island, our sample 19MU02, collected on the uneroded planeze (i.e. volcanic slope surface) of a lava flow, yielded an age of 84 ± 7 ka (Table 1), which is within uncertainty but much more precise than the previous $^{40}Ar/^{39}Ar$ plateau age of 40 ± 48 ka obtained for B6-3, also taken on the same planeze but from a borehole (Moore et al., 2011). Another sample of Moore et al. (2011), also coming from an outcrop on the same planeze, was dated by K–Ar on whole-rock at 1000 ± 25 ka (C76). This much older age is in striking disagreement with our K–Ar age on groundmass, with the $^{40}Ar/^{39}Ar$ plateau age, and with the uneroded morphology of the sampled planeze. This suggests that some K–Ar ages on whole-rock from the dataset of Moore et al. (2011) may be inaccurate, the reason why, together with the absence of details about the analytical procedures, and potassium and radiogenic argon contents, we do not consider them further in our interpretation.

South of the island, our sample 19MU07, collected in a lava flow located in the inner eastern flank of the Bassin Blanc crater, yielded a K–Ar age of 44 ± 5 ka (Table 1). The previous $^{40}Ar/^{39}Ar$ plateau age of 56 ± 36 ka obtained for M15 (Moore et al., 2011) from the same crater also yielded a comparable but much less precise value than our K–Ar age.

Fig. 4a shows that over the last 150 ka period, our six new ages between 113 ± 7 and 14 ± 3 ka, are all much more precise than the eight previous $^{40}Ar/^{39}Ar$ ages ranging from 138 ± 29 ka to 40 ± 48 ka (Moore et al., 2011). Even the whole-rock K–Ar age of 177 ± 7 ka (McDougall and Chamalaun, 1969) has a lower uncertainty. This can be explained by the low K_2O content (from 0.20 to 0.51%; Table 2) and the relatively high CaO content (about 10%; Fig. 2) of basalts from the Younger Series, making the interfering isotopes correction for irradiated samples dated with $^{40}Ar/^{39}Ar$ an additional source of uncertainties. The ^{39}Ar and ^{37}Ar recoil induced by the irradiation on the glassy part of the matrix could also affect the flatness of $^{40}Ar/^{39}Ar$ plateaus (Schaen et al., 2020). Unfortunately, no age spectra nor isochron plots are shown in Moore et al. (2011) to further investigate the effect of irradiation on these samples. On the other hand, the unspiked Cassignol-Gillot technique (Gillot et al., 2006) necessitates only the measurement of the natural ^{40}Ar and ^{36}Ar isotopes. Since it does not require irradiation of the sample prior to analysis, as needed to produce ^{39}Ar from ^{39}K for the $^{40}Ar/^{39}Ar$ technique, no recoil effects nor correction for reactor-induced production of ^{36}Ar from ^{40}Ca (e.g., McDougall and Harrison, 1999) is needed for K–Ar dating. The Cassignol-Gillot technique, developed for Quaternary volcanics, relies on the detection of a very small difference between the isotopic $^{40}Ar/^{36}Ar$ ratio extracted from the sample and the atmospheric aliquots ratio, allowing radiogenic argon contents as low as 0.1% to be detected (Quidelleur et al., 2001). It has been shown to be especially suitable for very young dating, with relatively small uncertainties, of lavas from different geodynamic settings, such as subduction (Gertisser et al., 2012; Ricci et al., 2017), intra-plate (Blard et al., 2005; Marques et al., 2019) or plate boundary (Quidelleur et al., 2022; Rusquet et al., 2023) volcanism, for instance. Together with these examples, our study of the latest activity of Mauritius illustrates that the unspiked Cassignol-Gillot K–Ar technique is especially suitable for dating low-K young volcanic lavas with a relatively high precision of only a few ka.

5.2. Morphology and chemistry of the terminal volcanism

Three of our four samples from the north of the island cluster in the range 120–80 ka (19MU02, 19MU03, and 19MU09), and all are located on the same planeze. Together with the $^{40}Ar/^{39}Ar$ ages, this suggests that most of the volcanic products forming the gently domed, uneroded surface of Mauritius have erupted during this interval. Nevertheless, our sample 19MU10 dated at 14 ± 3 ka implies that the northern part of the island remained active until the near Holocene. Further south, our sample 19MU14 is issued from the uneroded planeze of a lava flow downhill of the Bassin Blanc crater. This sample, dated at 52 ± 6 ka, has a similar age to 19MU07 (44 ± 5 ka), within uncertainty. However, 19MU07 and 19MU14 have contrasting trace element patterns (Fig. 3), implying that the crater and the lava flow forming the planeze belong to different volcanic events.

Overall, our new ages and literature data show that the N20°E axis of Mauritius remained a major active volcano-tectonic structure until ≤40 ka. Interestingly, the latest activity of Piton des Neiges volcano in Réunion Island also occurred along a N30°E rift zone (Chaput et al., 2017; Bénard et al., 2023) until about 27 ka (Gillot et al., 1994; Famin et al., 2022). This similar pattern for two eruptive centers distant of ~230 km suggests that a regional stress field controlled their terminal volcano-tectonics, dominated by a N20–30°E maximum horizontal stress.

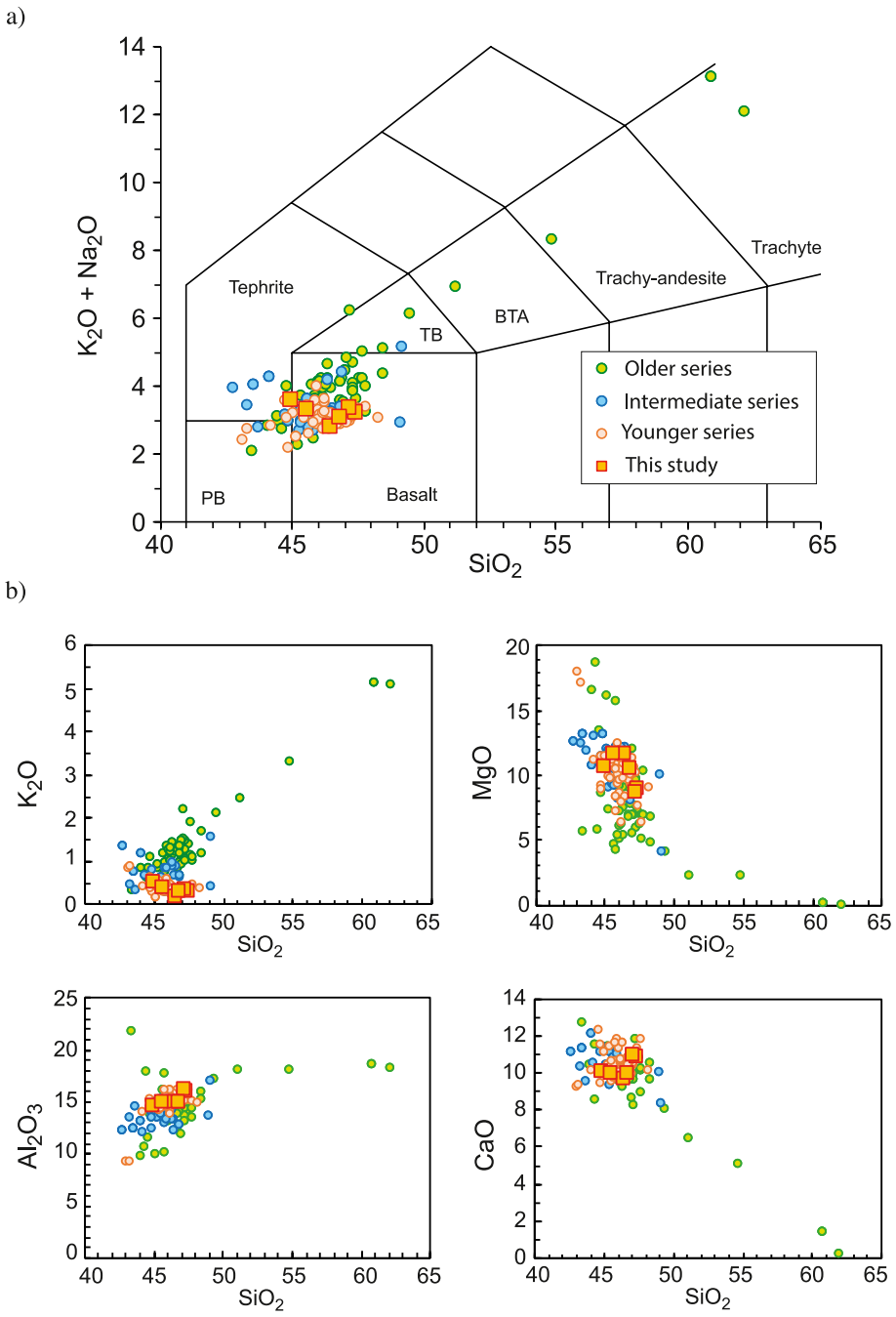

Fig. 2. Total alkali versus silica (TAS) diagram of rocks from Mauritius Island. Data have been extracted from the GEOROC database (see text for references). The large orange square symbols are for samples from this study. Samples from previous studies are shown with small circles with a given color for each volcanic series. Rock fields are from Le Bas et al. (1986). PB: Picro-basalt; B: Basanite; TB: Trachy-basalt; BTA: Basaltic trachy-andesite.

Another noticeable feature of erupted products for the past 150 ka is their exceptional homogeneity in major-trace element compositions, and their nearly constant depletion in incompatible elements on the lower half of the spectrum of the Younger series (Fig. 3). This homogeneity in depletion, contrasting with the end of the Older series and to a lesser extent with the Intermediate series, points to an absence of fractional crystallization or crustal assimilation of the emitted magmas, and hence to a rapid transfer from source to surface without any storage in-between. Incompatible element enrichments, due to partial melting decrease or fractional crystallization at shallow level, are generally a characteristic signature of fading magmatism, as observed in the Older series (e.g., Baxter, 1976; Ashwal et al., 2016) and on Piton des Neiges in Réunion (e.g., Kluska, 1997). The noteworthy absence of such a characteristic signature for the past 150 ka suggests that the rejuvenescent volcanism of the Younger series is not over.

5.3. *Implication volcanic hazards assessment*

In the Hawai'i archipelago, rejuvenescent volcanism initiated while the islands were about 100–200 km away from the plume head and remained active at distances of more than 500 km, as observed for Ka'ula, Ni'ihau and Kaua'i (Clague and Sherrod, 2014), on the Pacific plate moving at ~10 cm/yr above the plume (e.g., Wang et al., 2018). Given the slower motion of the Somali plate above the Réunion plume (~2.4 cm/yr toward the northeast, e.g., Wang et al., 2018), and given the ~200 km distance of Mauritius from the active eruptive center of

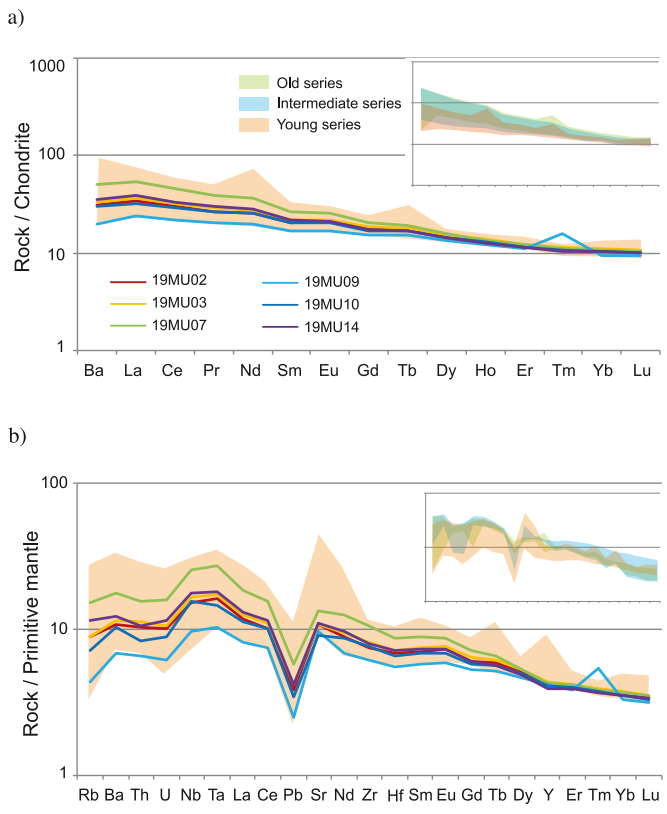

Fig. 3. a) Rare Earth Element (REE) patterns normalized to chondrite (after Sun and McDonough, 1989) of the samples used in this study. Beige color pattern indicates the range of data from GEOROC for the Younger Series. Insert: REE patterns of data from GEOROC for the Older (green), Intermediate (blue) and Younger (beige) Series. b) Same as a) for multi-element patterns normalized to primitive mantle (after Sun and McDonough, 1989).

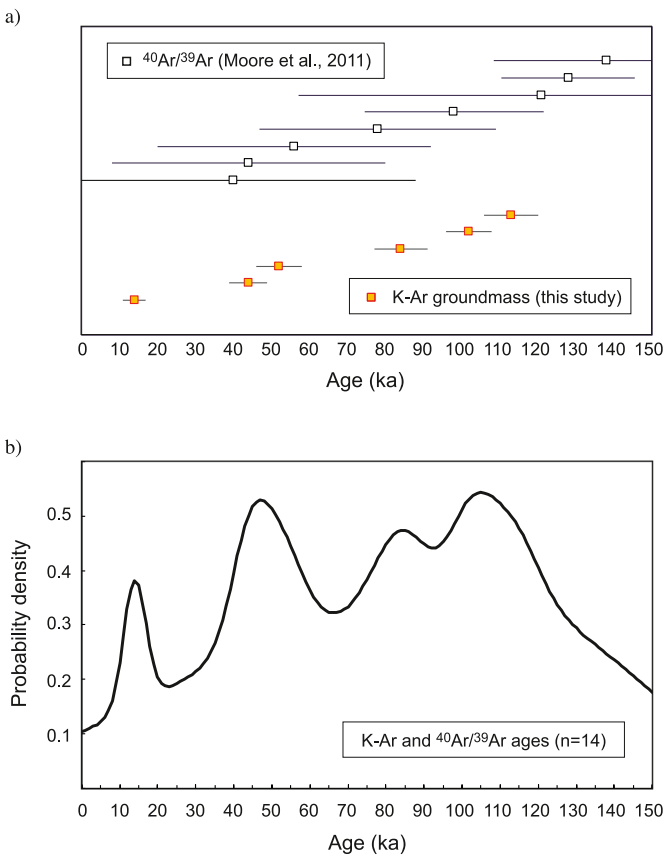

Fig. 4. a) K–Ar ages from this study (orange symbols) and $^{40}Ar/^{39}Ar$ ages from Moore et al. (2011; open symbols). b) Age-probability distribution spectrum (Deino and Potts, 1992) showing the periods of volcanic activity in Mauritius for the last 150 ka, based on ages shown in a).

Réunion Island, it can be envisioned by analogy with Hawai'i, that rejuvenescent volcanism in Mauritius may still be possible for several millions of years. Nevertheless, considering the relatively low production rate of the rejuvenescent magmatism, the probability that it will occur in the near future remains quite low.

The probability density (Fig. 4b) calculated for ages from Mauritius available for the 0–150 kyr interval, six K–Ar ages from this study (Table 1) and eight $^{40}Ar/^{39}Ar$ ages, suggest that volcanic activity was present throughout this interval all over the island (Fig. 1). Given the small uncertainty of our K–Ar ages, several periods of activity can be highlighted, at about 110, 85, 50 and 15 ka (Fig. 4b), with rest periods of about 20–40 kyr. As our near-Holocene age of 14 ± 3 ka (19MU10; Table 1) is younger than the duration of these apparent rest periods, it is possible that volcanism in Mauritius may resume at any time.

6. Conclusion

The new K–Ar groundmass and plagioclase ages obtained with the Cassignol-Gillot technique extend the Younger Series of Mauritius Island towards the near Holocene. They range from 113 ± 7 to 14 ± 3 ka, with a strongly improved precision compared to the $^{40}Ar/^{39}Ar$ ages previously available. Major and trace elements geochemistry of these basaltic lavas do not display marked differences with magmas emitted throughout the Younger Series, suggesting that magmatism remains in a steady state from source to surface since about 1 Myr. As no strong fractionation is evident, no fading of volcanism can be inferred for Mauritius Island.

This study demonstrates that Mauritius Island should be considered active and that volcanism can resume in the future. However, given the relatively low volume of the Younger Series and that only three periods of activity have been reported here since 100 ka, the probability of an eruption in the near future appears rather low.

Funding

Field trip and geochemistry analyses were funded by the LGSR, while GEOPS funded the K–Ar analyses.

CRediT authorship contribution statement

Xavier Quidelleur: Conceptualization, Formal analysis, Funding acquisition, Investigation, Writing – original draft, Writing – review & editing. **Vincent Famin:** Conceptualization, Formal analysis, Funding acquisition, Investigation, Methodology, Writing – original draft, Writing – review & editing.

Declaration of competing interest

The authors declare that they have no known competing financial interests or personal relationships that could have appeared to influence the work reported in this paper.

Data availability

Data will be made available on request.

Acknowledgements

C. Liorzou and B. Guégen from the University of Bretagne Occidentale are thanked for the major-trace element analyses. We also thank Irene Schimmelpfennig and an anonymous reviewer for their detailed reviews, constructive comments, and suggestions, which helped us to improve this manuscript. Valérie Godard is ackonwledged for having manufactured all the thin sections. This is LGMT contribution number 187.

Appendix A. Supplementary data

Supplementary data to this article can be found online at https://doi.org/10.1016/j.quageo.2024.101534.

References

Ashwal, L.D., Wiedenbeck, M., Torsvik, T.H., 2017. Archaean zircons in Miocene oceanic hotspot rocks establish ancient continental crust beneath Mauritius. Nat. Com 8, 14086.
Ashwal, L.D., Torsvik, T.H., Horváth, P., Harris, C., Webb, S., Werner, S., Corfu, F., 2016. A mantle-derived origin for Mauritian Trachytes. J. Petrol. 57, 1645–1676.
Baxter, A.N., 1972. Magmatic Evolution of Mauritius, Western Indian Ocean. PhD Thesis. Univ. of Edinburgh, Edinburgh, p. 177.
Baxter, A.N., 1975. Petrology of the older series lavas from Mauritius, Indian Ocean. Geol. Soc. Am. Bull. 86 (10), 1449–1458.
Baxter, A.N., 1976. Geochemistry and petrogenesis of primitive alkali basalt from Mauritius, Indian Ocean. Geol. Soc. Am. Bull. 87, 1028–1034.
Bénard, B., Famin, V., Sanjuan, B., Vimeux, F., Aunay, B., Agrinier, P., Lebeau, G., 2023. An integrated geochemical spatial and temporal survey of thermal springs to characterize the geothermal resource of a volcano (Piton des Neiges, Réunion Island). App. Geochem. 154, 105689.
Bianco, T.A., Ito, G., Becker, J.M., Garcia, M.O., 2005. Secondary Hawaiian volcanism formed by flexural arch decompression. Geochem. Geophys. Geosyst. 6, Q08009.
Blard, P.H., Lavé, J., Pik, R., Quidelleur, X., Bourlès, D., Kieffer, G., 2005. Fossil cosmogenic 3He record from K–Ar dated basaltic flows on Etna volcano (38°N): Evaluation of a new paleoaltimeter. Earth Planet Sci. Lett. 236, 613–631.
Carignan, J., Hild, P., Mevelle, G., Morel, J., Yeghicheyan, D., 2001. Routine analyses of trace elements in geological samples using flow injection and low pressure on-line liquid chromatography coupled to ICP-MS: a study of geochemical reference materials BR, DR-N, UB-N, AN-G and GH. Geostand. Newslett. 25 (2-3), 187–198.
Cassignol, C., Gillot, P.-Y., 1982. Range and Effectiveness of Unspiked Potassium-Argon Dating: Experimental Groundwork and Applications, vols. 159–179. John Wiley, New York.
Chaput, M., Famin, V., Michon, L., 2017. Sheet intrusions and deformation of Piton des Neiges, and their implication for the volcano-tectonics of La Réunion. Tectonophys 717, 531–546.
Clague, D.A., Sherrod, D.R., 2014. Growth and Degradation of Hawaiian Volcanoes: Chapter 3 in Characteristics of Hawaiian Volcanoes, vols. 1801–3. US Geological Survey, pp. 97–146.
Deino, A., Potts, R., 1992. Age-probability spectra for examination of single-crystal $^{40}Ar/^{39}Ar$ dating results: examples from Olorgesailie, southern Kenya Rift. Quat. Int. 13–14, 47–53.
Famin, V., Paquez, C., Danišík, M., Gardiner, N.J., Michon, L., Kirkland, C.L., Berrthod, C., Friedrichs, B., Schmiff, A.K., Monié, P., 2022. Multitechnique geochronology of intrusive and explosive activity on Piton des Neiges volcano, Réunion Island. Geochem., Geophys., Geosyst. 23 (5), e2021GC010214.
Fuhrmann, U., Lippolt, H.J., Hess, J.C., 1987. Examination of some proposed K–Ar standards: $^{40}Ar/^{39}Ar$ analyses and conventional K–Ar data. Chem. Geol. 66, 41–51.
Garcia, M.O., Swinnard, L., Weis, D., Greene, A.R., Tagami, T., Sano, H., Gandy, C.E., 2010. Petrology, geochemistry and geochronology of Kaua'i lavas over 4.5 Myr: implications for the origin of rejuvenated volcanism and the evolution of the Hawaiian plume. J. Petrol. 51, 1507–1540.
Garcia, M.O., Weis, D., Jicha, B.R., Ito, G., Hanano, D., 2016. Petrology and geochronology of lavas from Ka 'ula Volcano: implications for rejuvenated volcanism of the Hawaiian mantle plume. Geochim. Cosmochim. Act 185, 278–301.
Germa, A., Quidelleur, X., Labanieh, S., Chauvel, C., Lahitte, P., 2011. The volcanic evolution of Martinique Island: insights for the Lesser Antilles arc migration since the Oligocene. J. Volcanol. Geoth. Res. 208, 122–135.
Germa, A., Quidelleur, X., Shea, T., Ricci, J., 2023. Preservation of inherited argon in plagioclase crystals in the Lesser Antilles: implication for residence time after reservoir remobilization. In: Goldschmidt 2023 Conference. Lyon, France.
Gertisser, R., Charbonnier, S., Keller, J., Quidelleur, X., 2012. The geological evolution of Merapi volcano, Central Java, Indonesia. Bull. Volcanol. 74, 1213–1233.
Gillot, P.-Y., Cornette, Y., 1986. The Cassignol technique for Potassium-Argon dating, precision and accuracy: exemples from the late Pleistocene to recent volcanics from southern Italy. Chem. Geol. Isot. Geosci. Sect. 59, 205–222.
Gillot, P.-Y., Cornette, Y., Max, N., Floris, B., 1992. Two reference materials, trachytes MDO- G and ISH-G, for argon dating (K–Ar and $^{40}Ar/^{39}Ar$) of Pleistocene and Holocene rocks. Geostand. Newsl. 16, 55–60.
Gillot, P.-Y., Lefèvre, J.-C., Nativel, P., 1994. Model for the structural evolution of the volcanoes of Réunion Island. Earth Planet Sci. Lett. 122 (3–4), 291–302.
Gillot, P.-Y., Hildenbrand, A., Lefèvre, J.-C., Albore-Livadie, C., 2006. The K/Ar dating method: principle, analytical techniques, and application to Holocene volcanic eruptions in Southern Italy. Acta Vulcanol. 18, 55–66.
Giorgi, L., Borchiellini, S., Delucchi, L., 1999. Ile Maurice Carte Geologigue Notice Explicative, Water Resources Unit, Republic of Mauritius. Rose Hill, Mauritius.
Guillou, H., Torrado, F.J.P., Machin, A.R.H., Carracedo, J.C., Gimeno, D., 2004. The Plio-Quaternary volcanic evolution of Gran Canaria based on new K–Ar ages and magneto-stratigraphy. J. Volcanol. Geoth. Res. 135, 221–246.
Hanyu, T., Dunai, T.J., Davies, G.R., Kaneoka, I., Nohda, S., Uto, K., 2001. Noble gas study of the Reunion hotspot: evidence for distinct less-degassed mantle sources. Earth Planet Sci. Lett. 193 (1–2), 83–98.
Kluska, J.-M., 1997. Evolution magmatique et morpho-structurale du Piton des Neiges au cours des derniers 500 000 ans. Université Paris Sud, p. 246.
Konter, J.G., Jackson, M.G., 2012. Large volumes of rejuvenated volcanism in Samoa: evidence supporting a tectonic influence on late-stage volcanism. Geochem., Geophys., Geosyst. 13 (6).
Le Bas, M.J., Le Maitre, R.W., Streckeisen, A., Zanettin, B., IUGS Subcommission on the Systematics of Igneous Rocks, 1986. A chemical classification of volcanic rocks based on the total alkali-silica diagram. J. Petrol. 27, 745–750.
Marques, F.O., Hildenbrand, A., Victória, S.S., Cunha, C., Dias, P., 2019. Caldera or flank collapse in the Fogo volcano? What age? Consequences for risk assessment in volcanic islands. J. Volcanol. Geoth. Res. 388, 106686.
McDougall, I.A.N., Chamalaun, F.H., 1969. Isotopic dating and geomagnetic polarity studies on volcanic rocks from Mauritius, Indian Ocean. Geol. Soc. Am. Bull. 80 (8), 1419–1442.
McDougall, I.A.N., Harrison, T.M., 1999. Geochronology and Thermochronology by the $^{40}Ar/^{39}Ar$ Method. Oxford University Press, p. 269.
Montaggioni, L.F., Martin-Garin, B., 2020. Episodic coral growth events during the building of Reunion and Mauritius shield volcanoes (Western Indian Ocean). Facies 66 (3), 13.
Moore, J., White, W.M., Paul, D., Duncan, R.A., Abouchami, W., Galer, S.J., 2011. Evolution of shield-building and rejuvenescent volcanism of Mauritius. J. Volcanol. Geoth. Res. 207 (1–2), 47–66.
Morgan, W.J., 1981. Hotspot tracks and the opening of the atlantic and Indian oceans. In: Emiliani, C. (Ed.), The Sea: the Oceanic Lithophere. John Wiley and Sons, New York, pp. 443–487.
Nauret, F., Famin, V., Vlastélic, I., Gannoun, A., 2019. A trace of recycled continental crust in the Réunion hotspot. Chem.l Geol. 524, 67–76.
Nohda, S., Kaneoka, I., Hanyu, T., Xu, S., Uto, K., 2005. Systematic variation of Sr-, Nd- and Pb-isotopes with time in lavas of Mauritius, Réunion hotspot. J. Petrol. 46 (3), 505–522.
Paul, D., White, W.M., Blichert-Toft, J., 2005. Geochemistry of Mauritius and the origin of rejuvenescent volcanism on oceanic island volcanoes. Geochem., Geophys., Geosyst. 6 (6).
Paul, D., Kamenetsky, V.S., Hofmann, A.W., Stracke, A., 2007. Compositional diversity among primitive lavas of Mauritius, Indian Ocean: implications for mantle sources. J. Volcanol. Geoth. Res. 164 (1–2), 76–94.
Perroud, B., 1982. Etude volcano-structurale des îles Maurice et Rodrigues (Océan Indien Occidental). Origin du volcanisme. Thèse de Doctorat de Spécialité. Université de Grenoble, p. 210.
Quidelleur, X., Gillot, P.Y., Soler, V., Lefèvre, J.C., 2001. K–Ar dating extended into the last millennium: application to the the youngest effusive episode of the Teide volcano (Canary Islands, Spain). Geophys. Res. Lett. 28, 3067–3070.
Quidelleur, X., Michon, L., Famin, V., Geffray, M.-C., Danišík, M., Gardiner, N., Rusquet, A., Mohamed, Gou Z., 2022. Holocene volcanic activity in Anjouan Island (Comoros archipelago) revealed by new Cassignol-Gillot groundmass K–Ar and 14C ages. Quat. Geochron. 67, 101236.
Raczek, I., Stoll, B., Hofmann, A.W., Peter Jochum, K., 2001. High-precision trace element data for the USGS reference materials BCR-1. BCR-2, BHVO-1, BHVO-2, AGV-1, AGV- 2, DTS-1, DTS-2, GSP-1 and GSP-2 by ID-TIMS and MIC-SSMS. Geostand. Newslett. 25, 77–86.
Ricci, J., Quidelleur, X., Pallares, C., Lahitte, P., 2017. High-resolution K–Ar dating of a complex magmatic system: the example of Basse-Terre Island (French West Indies). J. Volcanol. Geoth. Res. 345, 142–160.
Rusquet, A., Famin, V., Quidelleur, X., Michon, L., Nauret, F., Danišík, M., 2023. Pliocene-to-Holocene volcano-tectonic activity on Mohéli Island (Comoros archipelago) constrained by new K–Ar ages. J. Volcanol. Geoth. Res. 442, 107896.
Saddul, P., 2002. Mauritius. A geomorphological analysis. Geography of Mauritius Series. Mahatma Gandhi Institute, p. 354.
Schaen, A.J., Jicha, B.R., Hodges, K.V., Vermeesch, P., Stelten, M.E., Mercer, C.M., Phillips, D., Rivera, T.A., Jourdan, F., Matchan, E.L., Hemming, S.R., Morgan, L.E., Kelley, S.P., Cassata, W.S., Heizler, M.T., Vasconcelos, P.M., Benowitz, J.A., Koppers, A.A.P., Mark, D.F., Niespolo, E.M., Sprain, C.J., Hames, W.E., Kuiper, K.F., Turrin, B.D., Renne, P.R., Ross, J., Nomade, S., Guillou, H., Webb, L.E., Cohen, B.A., Calvert, A.T., Joyce, N., Ganerød, M., Wijbrans, J., Ishizuka, O., He, H., Ramirez, A., Pfänder, J.A., Lopez-Martínez, M., Qiu, H., Singer, B.S., 2020. Interpreting and reporting $^{40}Ar/^{39}Ar$ geochronologic data. GSA Bulletin 133, 461–487.
Schwarz, W.H., Trieloff, M., 2007. Intercalibration of 40Ar–39Ar age standardsNL-25, HB3gr hornblende, GA1550, SB-3, HD-B1 biotite and BMus/2 muscovite. Chem. Geol. 242, 218–231.
Sheth, H.C., Mahoney, J.J., Baxter, A.N., 2003. Geochemistry of lavas from Mauritius, Indian Ocean: mantle sources and petrogenesis. Int. Geol. Rev. 45 (9), 780–797.
Simpson, E.S.W., 1950. The geology and mineral resources of Mauritius. Colon. Geol. Miner. Resour. 1, 217–238.

Steiger, R.H., Jäger, E., 1977. Subcommission on Geochronology: convention on the use of decay constants in Geo and Cosmochronology. Earth Planet Sci. Lett. 36, 359–362.
Sun, S.S., McDonough, W.F., 1989. Chemical and isotopic systematics of oceanic basalts: implications for mantle composition and processes. Geol. Soc. 42, 313–345. London, Special Publications.
Taylor, J.R., 1982. An Introduction to Error Analysis. University Science Books, p. 270. Mill Valley.
Wang, S., Yu, H., Zhang, Q., Zhao, Y., 2018. Absolute plate motions relative to deep mantle plumes. Earth Planet Sci. Lett. 490, 88–99.